The final version of this article is published by Superconductor Sci. Technol. (2010), see
http://iopscience.iop.org/0953-2048/23/6/065006.

Simplified Analysis of Direct SQUID Readout Schemes

D. Drung
Physikalisch-Technische Bundesanstalt (PTB),
Abbestrasse 2-12, D-10587 Berlin, Germany
E-mail: dietmar.drung@ptb.de

***Abstract* - A simple approach to understand and analyze direct readout schemes for Superconducting QUantum Interference Devices (SQUIDs) is presented. It is shown that the existing methods for suppression of room temperature amplifier noise are based on voltage feedback and current feedback in the SQUID that were introduced in the original schemes of additional positive feedback (APF) and bias current feedback (BCF). It is also shown that the way the SQUID is biased (at constant current or voltage) does not affect the noise suppression**.

Submitted February 19, 2010; accepted February 20, 2010. Reference No. ST188; Category 4.
The final version of this article is published by Superconductor Sci. Technol. (2010),
see http://iopscience.iop.org/0953-2048/23/6/065006.

Keywords – SQUID, readout, amplifier, noise, current feedback, voltage feedback; **PACS** 85.25.Dq

I. INTRODUCTION

To take the full advantage of its low intrinsic noise, the superconducting quantum interference device (SQUID) requires a low-noise room temperature amplifier [1,2]. Traditionally, SQUIDs were operated in a flux-locked loop (FLL) using a flux modulation technique [3]. Direct readout without flux modulation was introduced in the early 1990s as a way to simplify the readout electronics in biomagnetic multichannel systems. It has become more and more popular in the past decade, stimulated in part by the need of higher bandwidth and slew rate, *e.g.*, for the readout of cryogenic detectors. Various methods have been developed to suppress the effect of amplifier noise when using direct readout [4-11].

The basic components of direct SQUID readout are shown in Figure 1. The SQUID is basically a flux-to-voltage or flux-to-current converter, in which the applied flux Φ_a represents the input signal. The transfer characteristic is strongly nonlinear. It is periodic in flux with the period being the flux quantum Φ_0. The signal from the SQUID is amplified, integrated, and fed back into the SQUID loop via a feedback resistor R_F and a feedback coil that is magnetically coupled to the SQUID via a mutual inductance M_F. Commonly, the impedance of the feedback coil can be neglected because the feedback inductance is small and the feedback resistance is in the kΩ range. For infinite integrator gain, the flux in the SQUID is kept constant by the negative feedback, and the voltage V_F across the feedback resistor depends linearly on the applied flux. In some high-frequency applications, SQUIDs are alternatively read out in a small-signal mode without room temperature FLL. In this case, the integrator in Figure 1 is omitted, and the voltage at the amplifier output is used for the output signal. Direct-coupled FLL circuits are easily understood and designed; their behavior and analysis is well described in literature [1,2,4]. Therefore, we focus here on the analysis of the two crucial components: SQUID and amplifier.

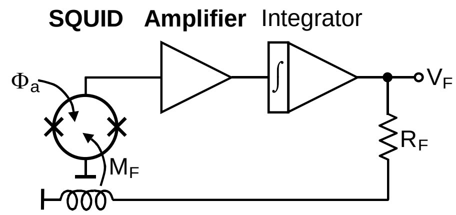

Fig. 1. Basic direct-coupled FLL circuit. A dc SQUID is drawn (circle with two crosses indicating the Josephson junctions), but any type of SQUID with nonhysteretic transfer characteristic can be used.

II. BASIC MODEL FOR SQUID AND AMPLIFIER

The basic equivalent circuit of a SQUID connected to an amplifier is depicted in Figure 2. All voltages (SQUID voltage V and output voltage V_{Out}) are referenced to ground. The SQUID is operated at cryogenic temperatures, while the amplifier is usually placed at room temperature. There is a typically 1 m long cable between SQUID and amplifier that is omitted in Figure 2 for clarity. Twisted wire pairs with a low heat load to the cryogenic part are commonly used, but for demanding wideband applications coaxial cables may be required.

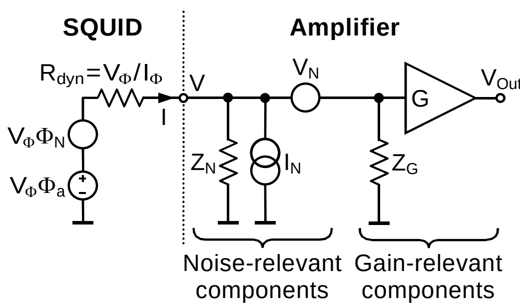

Fig. 2. Basic equivalent circuit of a SQUID/amplifier arrangement. The current I represents the load current flowing out of the SQUID into the amplifier.

The SQUID is modeled in Figure 2 by a resistance R_{dyn} plus two voltage sources that take into account the effects of the applied signal flux Φ_a and the intrinsic flux noise of the SQUID Φ_N. Depending on the use of the SQUID as magnetometer or current sensor, the applied flux Φ_a is generated by a magnetic field or by a current flowing through an input coil magnetically coupled to the SQUID. These details are not shown in Figure 2 for simplicity. There are two basic transfer coefficients: the *voltage* transfer coefficient $V_\Phi = \partial V/\partial \Phi_a$ that is measured at constant current I through the SQUID; correspondingly $I_\Phi = \partial I/\partial \Phi_a$ is the *current* transfer coefficient at constant voltage V across the SQUID. The SQUID is inherently a wideband device; therefore, the transfer coefficients V_Φ and I_Φ are assumed to be frequencyindependent within the frequency range of interest. If necessary, the frequency dependence can easily be considered. In this case, V_Φ and I_Φ become complex and the dynamic resistance $R_{\mathrm{dyn}} = V_\Phi/I_\Phi$ has to be replaced by complex impedance Z_{dyn}. Note that alternatively to I_Φ the current sensitivity $M_{\mathrm{dyn}} = 1/I_\Phi$ may be used as a figure of merit for current noise effects. Both parameters M_{dyn} and I_Φ have the same sign because the direction of the current I has been changed compared to [2,4]. In this paper, the current transfer coefficient I_Φ is used rather than the current sensitivity M_{dyn} to demonstrate the similarity of voltage and current feedback more clearly.

The amplifier is represented in Figure 2 by two noise sources V_{N} and I_{N} plus two input impedances and an ideal voltage amplifier with a voltage gain G. It is an important feature that the total input impedance Z_{In} of the amplifier is modeled by two impedances Z_{N} and Z_{G}, which are connected in parallel via the voltage noise source V_{N}:

$$Z_{\mathrm{In}} = Z_{\mathrm{N}} \,||\, Z_{\mathrm{G}} = \frac{1}{1/Z_{\mathrm{N}} + 1/Z_{\mathrm{G}}} \quad . \tag{1}$$

The impedance Z_{N} affects both the overall noise and gain. In contrast, Z_{G} influences the gain only but has no effect on the noise performance of the setup. Note that the impedances are generally frequency-dependent (complex).

The effect of amplifier noise can be described by an equivalent excess flux noise ΔS_Φ in the SQUID loop:

$$\Delta S_\Phi = \left|1 + R_{\mathrm{dyn}}/Z_{\mathrm{N}}\right|^2 S_V/V_\Phi^2 + S_I/I_\Phi^2 \quad . \tag{2}$$

Here, S_V and S_I are the power spectral densities of the voltage and current noise sources V_{N} and I_{N}, respectively. In case of frequency-dependent (complex) transfer coefficients, V_Φ^2 and I_Φ^2 have to be replaced by $|V_\Phi|^2$ and $|I_\Phi|^2$. Note that a finite impedance Z_{N} indeed increases the amplifier flux noise contribution ΔS_Φ. This results from the fact that the SQUID signal is reduced at the amplifier input due to the voltage divider effect of R_{dyn} and Z_{N}, which increases the amplifier voltage noise contribution. Therefore, at high frequencies the noise rises due to parasitic capacitances (cable, input transistors of the amplifier). In the extreme case $|Z_{\mathrm{N}}| \ll R_{\mathrm{dyn}}$ the total amplifier noise contribution becomes $\Delta S_\Phi = (S_V/|Z_{\mathrm{N}}|^2 + S_I)/I_\Phi^2$, *i.e.*, the amplifier voltage noise is equivalent to a virtual current noise with a spectral density $S_V/|Z_{\mathrm{N}}|^2$ [19]. In contrast, the amplifier current noise contribution S_I/I_Φ^2 is not affected by the input impedance.

Analysis of the basic circuit in Figure 2 yields the overall small-signal gain

$$\partial V_{\mathrm{Out}}/\partial \Phi_{\mathrm{a}} = \frac{G}{1/V_\Phi + 1/(I_\Phi Z_{\mathrm{In}})} \quad . \tag{3}$$

In general, the gain is influenced by both transfer coefficients V_Φ and I_Φ (denominator in Eq. (3)). For the limiting case $Z_{\mathrm{In}} \to \infty$ (ideal current bias) the gain is determined by V_Φ only, i.e., by the V-Φ_{a} characteristic. Correspondingly, for $Z_{\mathrm{In}} \to 0$ (ideal voltage bias) the gain is given by the I-Φ_{a} characteristic only.

Figures 1-2 represent a simplified, but nevertheless very useful model of a direct-coupled SQUID system. The basic modules SQUID and amplifier are involved, but neither extra circuitry for the suppression of amplifier noise nor components required to bias the

SQUID at constant current or voltage are shown. The essential idea of the analysis presented here is to separate all extra circuitry into SQUID-related and amplifier-related components. The real SQUID with noise reduction circuitry is then replaced by a basic SQUID with equivalent parameters. Similarly, the real readout amplifier is converted into a basic amplifier with equivalent parameters. Finally, these equivalent parameters are simply inserted into the equations derived for the basic circuit in Figure 2.

III. SQUID FEEDBACK TECHNIQUES

The main problem with direct readout is that the *voltage* noise level of even the best room temperature amplifiers is significantly higher than the noise of the bare SQUID, typically 100 pV/√Hz for a device operated at liquid helium temperature $T = 4.2$ K. Amplifier *current* noise is generally less critical, but it can become significant at low frequencies due to the relatively high 1/f current noise of the bipolar input transistors typically used for direct SQUID readout. At very high frequencies, the current noise usually increases due to capacitive effects and may even become the dominant noise source [12]. Various methods for suppressing the effect of amplifier noise are described in the literature [4-11]. They are all based on two fundamental feedback schemes, voltage feedback and current feedback (see Fig. 3).

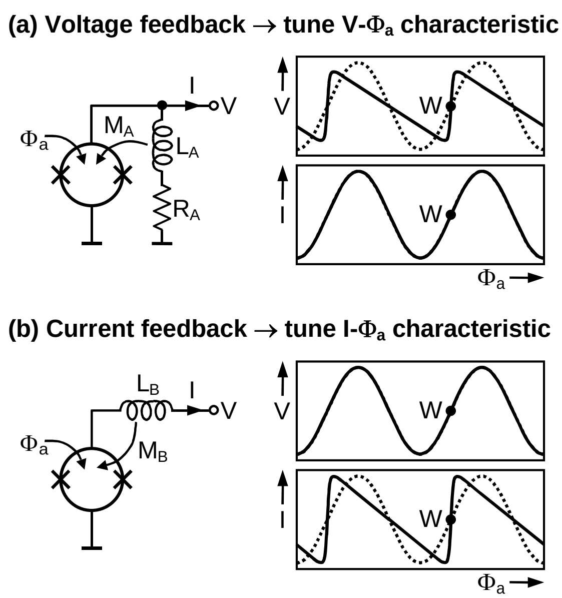

Fig. 3. Basic circuits for (a) voltage feedback and (b) current feedback. The corresponding SQUID characteristics with feedback (solid lines) and without feedback (dotted lines) are schematically depicted on the right side. With voltage feedback the swing in the V-Φ_a characteristic is reduced, whereas with current feedback the full swing is preserved in the I-Φ_a characteristic. The working point W is also shown for positive feedback.

Voltage feedback was first introduced for a current-biased SQUID under the name *additional positive feedback* (APF) [5]. Subsequently, it was applied to a voltage-biased SQUID [6] and named *noise cancellation* (NC) method [7]. The intention was to suppress the effect of preamplifier voltage noise to a level where it no longer dominates the overall noise.

Voltage feedback modifies the V-Φ_a characteristic and increases the transfer coefficient V_Φ at one slope, but does not affect the shape of the I-Φ_a characteristic. Neglecting the voltage across of the feedback coil L_A, the parameters of the equivalent SQUID (superscript A) at the working point W are given by:

$$V_\Phi^A = \frac{V_\Phi}{1-\beta_V} \quad , \quad I_\Phi^A = I_\Phi \quad , \quad S_\Phi^A = S_\Phi + 4k_B T R_A \left(\frac{\beta_V}{V_\Phi}\right)^2 \quad , \tag{4}$$

where

$$\beta_V = \frac{V_\Phi}{R_A}\left(M_A - \frac{1}{I_\Phi}\right) \tag{5}$$

is the voltage feedback coefficient. Here, k_B is the Boltzmann constant and T is the absolute temperature. The voltage swing in the V-Φ_a characteristic is reduced by the resistive load R_A. This effect is included in Eqs. (4) -(5), which yield a finite $\beta_V = -R_{dyn}/R_A$ and a correspondingly reduced $V_\Phi^A = V_\Phi/(1+R_{dyn}/R_A)$ when setting $M_A = 0$. Some excess noise occurs due to Nyquist noise in R_A. It is typically acceptable when R_A has the same operation temperature as the SQUID [2].

The feedback coefficient β_V determines the strength of the feedback effect. The sign of β_V defines whether positive or negative feedback occurs. Positive feedback increases the transfer coefficient V_Φ and lowers the amplifier voltage noise contribution at the expense of a degraded linear flux range. In contrast, negative feedback improves the intrinsic linearity of the SQUID. It is uncommon in practice for single SQUIDs due to the increased amplifier voltage noise contribution. A finite voltage drop across the feedback coil L_A causes a frequency dependence of the transfer coefficient V_Φ^A. The characteristic frequency is the 3-dB cut-off of the feedback circuit $f_A = R_A/(2\pi L_A)$. As usual, positive feedback leads to a bandwidth reduction. The frequency range with increased transfer coefficient ranges from dc to $(1-\beta_V) f_A$ [4]. For feedback coils integrated into the SQUID chip, the inductance L_A is typically low enough to neglect the frequency dependence of the transfer coefficient V_Φ^A in the frequency range of interest even for strong positive feedback.

The V-Φ_a characteristic becomes very steep if β_V approaches unity. Theoretically, an infinite transfer coefficient $V_\Phi^A \to \infty$ is obtained in the critical case $\beta_V = 1$, and hysteresis occurs in the V-Φ_a characteristic for $\beta_V > 1$. However, due to wideband noise effects, practical V-Φ_a characteristic are commonly "noise rounded" and the intrinsic hysteresis might be wiped out (in particular in the case of high-inductance SQUIDs with high current sensitivity). It can happen that the measured V-Φ_a characteristic appears useful but the observed noise is unexplainably high due to "invisible" high-frequency switching between the two stable regimes in the V-Φ_a characteristic. Another pitfall with voltage feedback is a too high feedback bandwidth, which may result in an increased SQUID noise level caused by mixed-down wideband noise. For example, for our SQUIDs with positive voltage feedback we observed that the intrinsic flux noise rises if f_A exceeds about 100 MHz [13]. Note that wideband noise may also reduce the transfer coefficients at high values of the FLL bandwidth. Therefore, it is best to measure V_Φ and I_Φ directly in the FLL mode with nominal system settings. For this, small test signals are superimposed to the SQUID bias voltage or bias current, and the resulting flux change is determined from the FLL output signal. This feature is included in modern wideband SQUID electronics (for example [14,15]).

An effect similar to voltage feedback can be obtained by making the shunt resistors of the junctions in the SQUID strongly asymmetric [10]. In a simplified view, the asymmetry in the junction shunts acts as a virtual feedback resistance R_A and the SQUID inductance L is used for the feedback coil L_A. Note that there are other alternatives to obtain a large voltage transfer coefficient, *e.g.*, the use of series SQUID arrays [16], SQUIDs with weakly shunted Josephson junctions operated near the hysteresis limit [14, 17] or SQUIDs with unshunted junctions based on relaxation oscillations [2,18]. The V-Φ_a characteristic remains symmetric in these cases. However, similar to voltage feedback the dynamic resistance increases with the voltage transfer coefficient, so that the current transfer coefficient remains unchanged (series SQUID arrays) or changes only weakly. Consequently, amplifier current noise effects should not be neglected *a priori* in theses devices.

The scheme of current feedback is shown in Figure 3(b). It was introduced under the name *bias current feedback* (BCF) as a measure to suppress amplifier current noise [8]. Complementary to voltage feedback, current feedback modifies the I-Φ_a characteristic but does not affect the shape of the V-Φ_a characteristic. Neglecting the voltage across the feedback coil L_B, the parameters of the equivalent SQUID (superscript B) at the working point W are given by:

$$V_\Phi^B = V_\Phi \quad , \quad I_\Phi^B = \frac{I_\Phi}{1-\beta_I} \quad , \quad S_\Phi^B = S_\Phi \quad , \tag{6}$$

where

$$\beta_I = I_\Phi M_B \tag{7}$$

is the current feedback coefficient. In contrast to voltage feedback, there is no reduction in the current swing and no excess flux noise. However, wideband noise effects may distort the SQUID characteristic similar to the case with voltage feedback (in particular for sensitive high-inductance SQUIDs). It is advisable to connect a resistor R_B in parallel with the feedback coil L_B in order to avoid a too high feedback bandwidth [8]. The small amount of extra Nyquist noise in R_B is typically acceptable.

The sign of β_I determines whether positive or negative feedback occurs. Current feedback was originally introduced to reduce the effect of amplifier current noise (positive feedback). Asymmetric bias current feed has a similar effect as current feedback; here, half of the SQUID inductance L acts as a virtual feedback coil leading to an effective $M_B = \pm L/2$ [9]. Recently, negative current feedback was used to increase the linearity when operating a SQUID (array) without room temperature FLL. This technique was called *output current feedback* (OCF) [19] or *current-sampling feedback* [20]. It requires a current amplifier described in the next section.

Equations (4)-(7) show that voltage and current feedback are complementary with respect to their effect on the basic SQUID parameters V_Φ, I_Φ and S_Φ. If the two feedback schemes are combined, it plays no significant role which feedback is done first. Figure 4(a) shows the original double feedback scheme [8], where first voltage feedback is performed and the resulting modified SQUID (circuit inside dashed box) is equipped with current feedback.

The circuit in Figure 4(b) with the reversed order was recently presented in conjunction with voltage bias as a *SQUID bootstrap circuit* (SBC) [11]. The feedback in Figure 4(b) may alternatively be realized by using only one coil with a tap instead of two separate coils L_A and L_B.

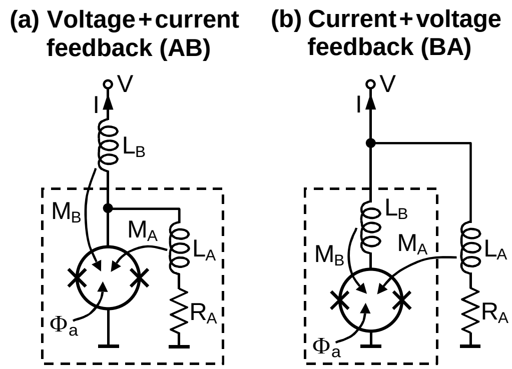

Fig. 4. Basic cascades of voltage and current feedback. The inner feedback loops are enclosed by dashed boxes.

Both circuits in Figure 4 show an equivalent voltage transfer coefficient and an increased flux noise level according to Eq. (4) as well as an equivalent current transfer coefficient according to Eq. (6). The feedback coefficients are found to be:

$$\beta_V^{AB} = \frac{V_\Phi}{R_A}\left(M_A - \frac{1}{I_\Phi}\right) \quad , \quad \beta_V^{BA} = \frac{V_\Phi}{R_A}\left(M_A + M_B - \frac{1}{I_\Phi}\right) \quad ,$$

$$\beta_I^{AB} = \beta_I^{BA} = I_\Phi M_B \quad (8)$$

Here, the superscripts AB and BA denote the order of the applied feedback schemes. The current feedback coefficients are identical, but the voltage feedback coefficients differ. In the case BA, both coils L_A and L_B contribute to the voltage feedback, whereas in the case AB only L_A is effective. However, this difference can be compensated by an adequate selection of the mutual inductance M_A. Consequently, for both cases identical voltage feedback coefficients can be chosen and the same overall SQUID performance is achievable.

There are other variants of voltage and current feedback reported in literature. In [8], only one feedback coil is used for both voltage and current feedback, and the feedback resistance R_A is merged into the junction shunt resistors. This circuit requires a more complex analysis, but the basic behavior is equivalent to the configurations in Figure 4. A special voltage bias scheme for the AB configuration was suggested in [4], where the feedback coil L_B suppresses amplifier current noise but does not reduce the linear flux range of the I-Φ_a characteristic as in the standard case. This results in an improved slew rate at a given system bandwidth. The scheme requires an extra wire between SQUID and amplifier, which makes the analysis somewhat more complicated than for the setups in Figure 4.

Current feedback can also be applied to a two-stage SQUID shown in Figure 5. This was demonstrated in [13] for the purpose of amplifier noise suppression under the somewhat misleading acronym APF (this acronym was used to point out that the additional feedback in the SQUID circuit is positive, rather than considering APF as a synonym for voltage feedback). In a two-stage setup, the weak SQUID signal is amplified by another SQUID before being passed to the room temperature amplifier. The signal flux Φ_a is applied to the first stage (the sensor SQUID) which is commonly voltage-biased by making the bias resistance much smaller than its dynamic resistance ($R_{Bias} \ll R_{dyn}$). The output of the sensor SQUID is inductively coupled to the second stage (the amplifier SQUID). Any type of SQUID may be used for the amplifier, but a series SQUID array is the preferable choice [2].

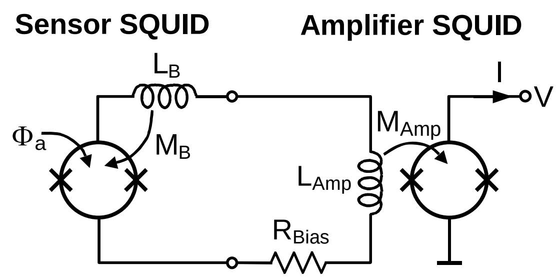

Fig. 5. Basic circuit of a two-stage SQUID with current feedback. The bias voltage for the sensor SQUID is generated by passing an appropriate current through the bias resistance R_{Bias}.

We first discuss the case without current feedback ($M_B = 0$). An important figure of merit is the flux gain at low frequencies

$$G_\Phi = \partial\Phi_{Amp}/\partial\Phi_a = \frac{M_{Amp}}{R_{Bias}/V_\Phi + 1/I_\Phi} \quad . \tag{9}$$

Here, V_Φ and I_Φ are the intrinsic transfer coefficients of the sensor SQUID and Φ_{Amp} is the flux coupled into the amplifier SQUID via the mutual inductance M_{Amp}. The loop consisting of sensor SQUID, bias resistance R_{Bias} and amplifier input inductance L_{Amp} forms an L-R low-pass. The flux gain falls above the cut-off frequency $f_{Amp} = (R_{dyn}+R_{Bias})/[2\pi(L_{Amp}+L_B)]$. The transfer coefficients of the two-stage SQUID are equal to those of the amplifier SQUID alone multiplied by the flux gain: $G_\Phi V_{\Phi,Amp}$ and $G_\Phi I_{\Phi,Amp}$. The amplifier SQUID causes an input-referred excess flux noise $\Delta S_\Phi = S_{\Phi,Amp}/G_\Phi^2$. Therefore, for a sufficiently high flux gain the noise contributions from the amplifier SQUID and from the room temperature amplifier become negligible, and the overall noise is dominated by the sensor SQUID even if it is operated at millikelvin temperatures. However, for high flux gains $G_\Phi \gg 1$ extra periods with non-equivalent working points appear in the overall characteristic of the two-stage SQUID because a flux modulation of one flux quantum in the sensor SQUID produces a large number of flux quanta in the amplifier SQUID.

Using current feedback, the flux gain can be increased in the vicinity of the nominal working point while obtaining an overall characteristic which looks essentially like that of a single SQUID [13]. The low-frequency flux gain with current feedback is given by

$$G_\Phi^B = \frac{G_\Phi}{1-\beta_I} \quad \text{with} \quad \beta_I = G_\Phi \frac{M_B}{M_{Amp}} \quad . \tag{10}$$

As in the previous cases, the sign of β_I defines whether positive feedback (amplifier noise suppression) or negative feedback (improved linearity) occurs. Positive feedback lowers the bandwidth, whereas negative feedback increases it. The cut-off frequency with current feedback is equal to $(1-\beta_I) f_{Amp}$.

This section is closed with a comment on noise impedance matching. Generally, it is assumed that minimum overall noise occurs if the dynamic resistance R_{dyn} of the SQUID is matched to the optimum source resistance $R_{opt} = (S_V/S_I)^{1/2}$ that minimizes the amplifier noise temperature [1]. In case of flux-modulated systems, this is indeed true; here, impedance matching is done via the ratio of the transformer turns placed between SQUID and amplifier. In the case of direct readout, one could intuitively think that it is best to perform a similar impedance matching by tuning the dynamic resistance via the voltage/current feedback parameters. However, this is not correct and leads to sub-optimum results.

Assume for example that the optimum amplifier impedance R_{opt} is given and that voltage feedback is applied to the SQUID. The feedback resistance R_A is selected to trade off excess noise against resistive load effect. According to Eqs. (4)-(5), the voltage transfer coefficient can be tuned via the mutual inductance M_A with minor effect on the SQUID noise (the feedback coefficient β_V remains near unity). The amplifier noise contribution is minimized by maximizing the voltage transfer coefficient $V_\Phi^A \to \infty$. As the current transfer coefficient I_Φ^A is not affected by voltage feedback, the resulting dynamic resistance $R_{dyn}^A = V_\Phi^A/I_\Phi^A$ also approaches infinity. Thus, minimum overall noise is found for an "impedance mismatch" $R_{dyn}^A \gg R_{opt}$. On the other hand, if voltage and current feedback are combined, minimum overall noise is found by maximizing both the voltage transfer coefficient and the current transfer coefficient. In practice, for optimized devices nearly zero dynamic resistance can be obtained [8] leading to an "impedance mismatch" $R_{dyn}^{AB} = R_{dyn}^{BA} \ll R_{opt}$. This demonstrates that in case of direct readout traditional noise impedance matching is not appropriate. Rather, the effects of amplifier voltage and current noise should be considered individually when optimizing the SQUID design.

IV. AMPLIFIER CONFIGURATIONS

The amplifier can be configured to measure the SQUID voltage or current as a function of the applied flux. These two basic amplifier concepts are depicted in Figure 6. For simplicity, the intrinsic amplifier input impedance is assumed to be infinite. The equivalent circuit of the voltage amplifier is quite simple, just consisting of a voltage and current noise source plus an ideal amplifier with voltage gain G. In contrast, the equivalent circuit of the current amplifier has a finite input impedance as a result of the feedback resistance R and the amplifier gain $-G$ (a negative gain is required for stability). Nyquist noise in R can be taken into account by increasing the spectral density of the amplifier current noise source I_N correspondingly ($\Delta S_I = 4k_BT/R$). Usually, a large resistance $R \gg R_{dyn}$ is chosen so that the flux noise contribution of the noise-relevant input impedance Z_N can be neglected according to Eq. (2). Consequently, the impedance $Z_G = R/G$ is the only difference between voltage and current amplifier. As Z_G does not affect the noise performance, both types of amplifiers yield the same overall noise. However, the current amplifier provides finite input impedance that can be used to terminate the cable between SQUID and amplifier [14].

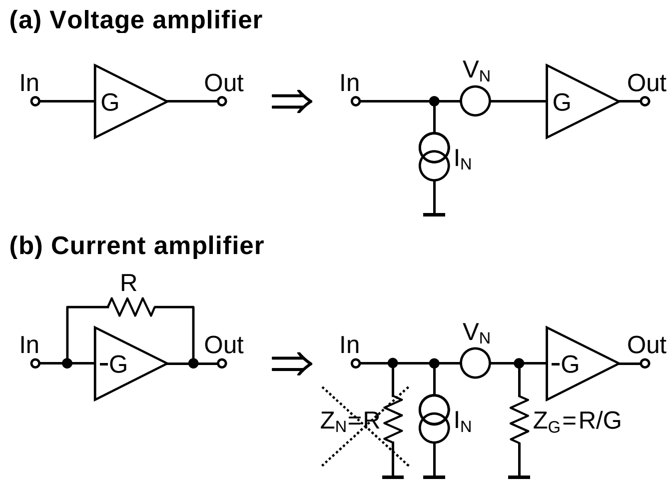

Fig. 6. Basic amplifier configurations and their equivalent circuits.

To provide ideal voltage bias at low frequencies, the amplifier in Figure 6(b) is replaced by an integrator (operational amplifier with dominant pole). This can be considered in the analysis by using a frequency-dependent amplifier gain $G = (\mathrm{j}\,f/f_1)^{-1}$, where f is the frequency, f_1 is the unity-gain frequency, and j is the imaginary unit. The resulting gain-relevant input impedance Z_G increases linearly with frequency, *i.e.*, it can be modeled by a virtual input inductance $L_G = R/(2\pi f_1)$. At low frequencies, the input impedance becomes sufficiently small to ensure voltage bias: $|Z_G| \ll R_{dyn}$. With voltage bias, the intrinsic linearity is improved [20] and consequently a higher slew rate at given bandwidth is achieved [4]. However, at high frequencies in the MHz range the inductive input is critical because it may interact with the cable connecting the SQUID with the amplifier. This may lead to *L-C* resonance effects. For wideband systems, it is preferable to design the amplifier such that the input impedance becomes resistive above about 10 MHz, with a value near the characteristic impedance of the cable.

At high frequencies, the intrinsic input impedance (capacitance) of the amplifier is no longer negligible and should be taken into account according to the model in Figure 2. The input impedance has to be split into noise-relevant and gain-relevant components depending on whether the effect is caused by shunt impedance (transistor input capacitance) or by a feedback mechanism (feedback capacitance between output and input of the first transistor stage). The overall noise performance of the SQUID system may not be predicted accurately if only the total amplifier input impedance Z_{In} is known.

The SQUID voltage/current bias sources are not explicitly considered in the simple model. However, their effect can easily be taken into account by increasing the power spectral densities of the voltage/current noise sources in Figure 2 appropriately. Finite source impedance can be included in the existing model impedances.

V. CONCLUSIONS

It was shown that direct SQUID readout schemes can be conveniently analyzed by considering SQUID and amplifier separately. This approach allows an intuitive understanding of the various readout concepts reported in literature, and leads to simple mathematical expressions for the expected overall behavior. Amplifier noise suppression can be performed by feeding the SQUID voltage and/or current back into the SQUID loop. These two basic concepts were first published in the early 1990s under the acronyms APF and BCF, and were demonstrated together in one magnetometer circuit. Since that time, a variety of noise reduction and linearization schemes based on voltage/current feedback was published. In the progress of circuit development, different terms evolved naturally resulting in the existing diversity of notation. This is confusing for newcomers in the field, and it would clearly be helpful if a common terminology for the various concepts could be established. This was attempted by Kiviranta, who introduced the terms “voltage-sampling feedback” and “current-sampling feedback” [20] which are more in line with the general circuit theory. However, in my opinion the expression “sampling” could be misunderstood, for which reason the terms “voltage feedback” and “current feedback “ are preferable.

Depending on the SQUID bias mode (constant current or voltage), the room temperature amplifier should be configured as a voltage or current amplifier. Current bias is more straightforward, but voltage bias yields a better intrinsic linearity of the SQUID and, correspondingly, a better slew rate at given bandwidth. For wideband systems, the amplifier should be designed such that the cable between SQUID and amplifier is terminated or (at least) resistively shunted. This means that at high frequencies there is neither ideal current bias nor ideal voltage bias present, but rather a mixture of both. The two elementary amplifier configurations (voltage/current amplifier) can be treated with the same equivalent circuit. There is no difference in the amplifier flux noise contribution, leading to identical overall noise levels for SQUIDs with current or voltage bias. As a result, the SQUID bias mode can be selected independently from the noise optimization according to the requirements in dynamic range and linearity.

ACKNOWLEDGEMENT

The author thanks Alex Braginski and Yi Zhang for stimulating this work and for fruitful discussions.

REFERENCES

[1] D. Drung “High-T_c and low-T_c dc SQUID electronics” *Supercond. Sci. Technol.* **16** 1320–1336 (2003).

[2] D. Drung and M. Mück “ SQUID electronics”. In *The SQUID Handbook* vol. l, J. Clarke and A. I. Braginski (Eds.), Wiley-VCH, Weinheim, pp. 127-170 (2004).

[3] J. Clarke, W.M. Goubau and M.B. Ketchen “Tunnel junction dc SQUID: fabrication, operation, and performance” *J. Low Temp. Phys.* **25** 99-144 (1976).

[4] D. Drung “Advanced SQUID read-out electronics”. In *SQUID Sensors: Fundamentals, Fabrication and Applications*, H. Weinstock (Ed.) NATO ASI Series E329,Kluwer Pbl., pp. 63-116.

[5] D. Drung, R. Cantor, M. Peters, *et al*. “Low-noise high-speed dc superconducting quantum interference device magnetometer with simplified feedback electronics”, *Appl. Phys. Lett.* **57** 406-408 (1990).

[6] H. Seppä, A. Ahonen, J. Knuutila *et al*. “dc-SQUID electronics based on adaptive positive feedback: experiments”, *IEEE Trans. Magn.* **27** 2488-2490 (1991).
[7] M. Kiviranta and H. Seppä “dc SQUID electronics based on the noise cancellation scheme”, *IEEE Trans. Appl. Supercond.* **5** 2146-2148 (1995).
[8] D. Drung and H. Koch “An electronic second-order gradiometer for biomagnetic applications in clinical shielded rooms”, *IEEE Trans. Appl. Supercond.* **3** 2594-2597 (1993).
[9] G. Uehara, N. Matsuda, K. Kazami *et al.* “Asymmetric bias injection technique for Drung-type superconducting quantum interference devices”, *Jpn. J. Appl. Phys.* **32** L1735-L1738 (1993).
[10] G. Testa, C. Granata, C. Di Russo *et al.* “Low-noise magnetometers with asymmetric superconducting quantum interference devices”, *Appl. Phys. Lett.* **79** 3989-3991(2001).
[11] X. Xie, Y. Zhang, H. Wang *et al.* “Voltage biased superconducting quantum interference device bootstrap circuit”, *Supercond. Sci. Technol.* (submitted on January 11, 2010).
[12] D. Drung, S. Bechstein, K.P. Franke *et al.* “Improved direct-coupled dc SQUID read-out electronics with automatic bias voltage tuning” *IEEE Trans. Appl. Supercond.* **11** 880-883 (2001).
[13] D. Drung, C. Aßmann, J. Beyer *et al.* “Highly sensitive and easy-to-use SQUID sensors”, *IEEE Trans. Appl. Supercond.* **17** 699-704 (2007).
[14] D. Drung, C. Hinnrichs and H.-J. Barthelmess “Low-noise ultra-high-speed dc SQUID readout electronics, *Supercond. Sci. Technol.* **19** S235–S241 (2006).
[15] SQUID electronics SEL-1 or XXF-1 from Magnicon GmbH, Lemsahler Landstr. 171, D-22397 Hamburg, Germany; http://www.magnicon.com.
[16] R.P. Welty and J. Martinis “A series array of dc SQUIDs” *IEEE Trans. Magn.* **27** 2924-2946 (1991).
[17] V. Polushkin, D. Glowacka, R. Hart and J. Lumley “Effect of an input coil microwave resonance on dynamics and noise properties of a dc superconducting quantum interference device operating close to the hysteretic mode”, *Rev. Sci. Instrum.* **70** 1713-1718 (1999).
[18] D.J. Adelerhof, H. Nijstad, J. Flokstra and H. Rogalla “(Double) relaxation oscillation SQUIDs with high flux-to-voltage transfer: simulations and experiments”, *J. Appl. Phys.* **76** 3875-3886 (1994).
[19] D. Drung, J. Beyer, M. Peters *et al.* “Novel SQUID current sensors with high linearity at high frequencies *IEEE Trans. Appl. Supercond.* **19** 772-777 (2009).
[20] M. Kiviranta “SQUID linearization by current-sampling feedback”, *Supercond. Sci. Technol.* **21** 045009 (2008).